IX CONGRESSO BRASILEIRO DE ENGENHARIA E CIÊNCIAS TÉRMICAS

9th BRAZILIAN CONGRESS OF THERMAL ENGINEERING AND SCIENCES

Paper CIT02-0599

DESIGN AND DEVELOPMENT OF A 70 N THRUST CLASS TURBOJET ENGINE

P. E. Trazzi
Rua Tiradentes, 427
09541-220, São Caetano do Sul - SP, Brazil
pgtrazzi@hotmail.com

Abstract. *Small turbojet engines are being used for propulsion of radio-controlled model airplanes. The design and development of the model 505 small jet engine are reviewed. Small size gas turbines present special design and construction difficulties, some of which are addressed; design choices leading to the final configuration are discussed. Aero-thermodynamic aspects are covered along with experimental data when available. The unit is comprised of a radial compressor, an annular combustion chamber, and an axial turbine plus accessories; details on these components and on production aspects are presented.*

Keywords: *gas turbines, jet propulsion, centrifugal compressors, combustors, axial flow turbines.*

1. Introduction

Small turbojet engines suitable for propulsion of model aircraft began to appear over the last decade. Concurrently, the studies, design and development of the unit presented here have begun. Regardless of size, gas turbines are subjected to high peripheral rotor speeds, high temperatures and hence high temperature differentials and stresses of high magnitude specially at the rotating assembly. As far as small units are considered, lower component efficiencies, tight tolerances and clearances, and accessories that don't scale in size or weight are some of the issues to be faced by the designer.

For this project general specifications were:

- Thrust rating 55-75 N
- Overall diameter 100 mm
- Life 200 h; 50,000 cycles
- Moderate fuel consumption
- Rugged design, yet weight below 1.3 kg
- Simple maintenance
- Superior safety features

During the study and design phases thrust figures were pushed toward the higher values shown, and space already exists allowing for further increases. A series of other detail modifications were carried out as early tests were conducted; the resulting prototype can be seen in Fig. (1).

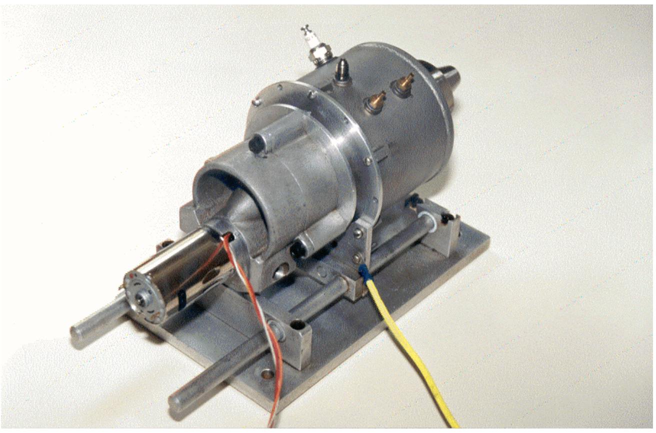

Figure 1. External view of the engine.

2. Overall performance and cycle analysis

Having a specified thrust rating, thermodynamic cycle analysis was made which yielded knowledge of mass flow and fuel consumption figures from values of specific thrust (thrust per unit mass flow) and specific fuel consumption, SFC (fuel flow per unit thrust). In Fig. (2) are plotted contours of constant specific thrust and SFC for a wide range of pressure ratios and turbine entry temperature, with compressor isentropic efficiencies likely to be encountered in such small units.

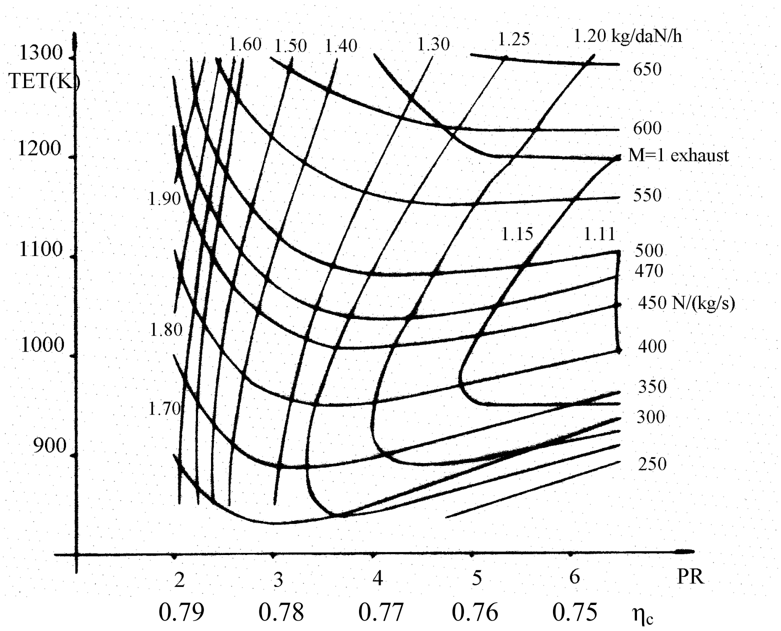

Figure 2. Contours of constant specific thrust and SFC.

Figure (2) shows that specific thrust is improved at higher turbine entry temperatures (TET), resulting in a smaller unit, while operation at higher pressure ratios tend to improve fuel economy. TET is limited by nozzle and turbine blade materials and life requirements. Higher compressor pressure ratios require higher rotor tip speeds, aluminum alloy rotors being usually limited around 4:1, beyond that only high-strength steels or titanium alloys being capable of withstanding the resulting centrifugal and thermal loads.

For the present design, compressor pressure ratio was largely determined by critical speed and bearing speed limitations. TET was fixed at 1100 K, allowing uncooled operation of nickel alloy IN713. The selected temperature level still allows for future rating growth to take place simply by increasing TET at the cost of a slight increase in SFC. To cope with the thrust requirement, a mass flow of 0.155 kg/s was selected. A complete summary of cycle parameters appears in Tab. (1).

Table 1. Design point performance parameters, static sea level, standard atmosphere.

Rotational speed, rpm	130,000
Mass flow, kg/s	0.155
Compressor Pressure Ratio	2.7
Compressor Efficiency, Total-Total	0.79
TET, K	1100
Exhaust Gas Temperature (EGT), K	998
Combustor Pressure Loss, $\Delta P_t/P_t$	0.05
Turbine Efficiency, Total-Total	0.80
Thrust, N	74
SFC, kg/daN/h	1.45

3. General layout

The gas turbine engine gives to the designer considerable freedom regarding the choice of the arrangement of the unit; having making the choice in favor of the centrifugal compressor, it is necessary to decide then the type and relative position of the turbine driving the compressor rotor, type and placement of the combustion chamber, bearings and accessories, if any. Figure (3) displays three possible layouts for the unit considered.

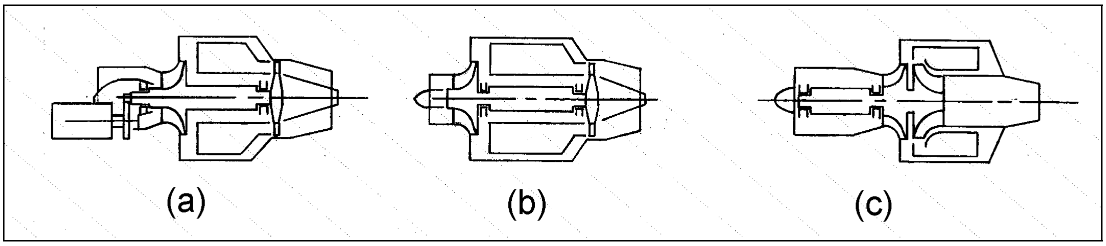

Figure 3. Layout of small gas turbines.

Layout (a); the one chosen for the present unit; has the compressor rotor between the two bearings, an axial flow turbine, although a radial turbine could also be employed and an annular combustion chamber. This layout permits the installation of a reduction unit to drive the accessories, which comprises, in this case, a starter/generator unit. Fuel and oil pumps are not shaft driven, the former being driven by a DC permanent magnet motor and the later being pressurized by compressor delivery air. Layout (b), currently employed by several model turbine manufacturers has a simple bearing arrangement, with the two bearing supported by a single part, making easier to obtain very tight concentricity between the two bearings; this layout also permits greater length for the combustion chamber before the shaft-rotor system encounters the first (bending) critical speed. On the other hand the installation of a reduction unit at the compressor end is not recommended because the bearing is located at the other side of the compressor rotor. Layout (c), with the rotors in a back-to-back arrangement, is widely employed in both jet propulsion and shaft power units, though limited to radial flow turbines; this layout allows cooler operation of both bearings. Units of this type operate, however, always at supercritical speeds, frequently employing, in at least one of the two bearings, some sort of resilient support for lower amplitudes of vibration to be found at the critical speed(s). Annular combustors but also single can; appropriate for shaft power units, being clearly unsuitable for jet propulsion units; combustors are found when examining units with this layout.

4. Compressor section

As pointed out in the cycle analysis section, aluminum alloy rotors are limited to a compression ratio of approximately 4:1, but for reasons other than centrifugal loads, compression ratio became limited at 2.7:1 in this project. Early during the study phase, computations began with a radial bladed rotor, because of the higher pressure ratios attainable with this kind of rotor, despite a somewhat lower isentropic efficiency and the fact that the peak efficiency usually founds itself very close to the surge margin. Later, with the selection of one of-the-shelf turbocharger rotor featuring sweptback blades, compression ratio was fixed at the above value. Actually sweptback rotors giving slightly less pressure at greater efficiencies almost offset the higher pressures at the lower efficiencies of the radial bladed rotor when computing specific thrust and SFC.

Detailed aerodynamic analysis of the compressor rotor and diffuser requires prior knowledge of compressor efficiency (η) and rotor slip factor (σ), as emphasized, for example, in Rodgers (1964). The former is best done by comparison with similar rotors in size and geometry; pressure ratio has some effect in efficiency, as higher speeds are approached, shock losses begin to occur; specific speed (Ns) can also affect efficiency, the range between 7-9 (95-120 in U.S. customary units) considered by some authors and verified by some experiment, to be where efficiency peaks; see Fig. (4).

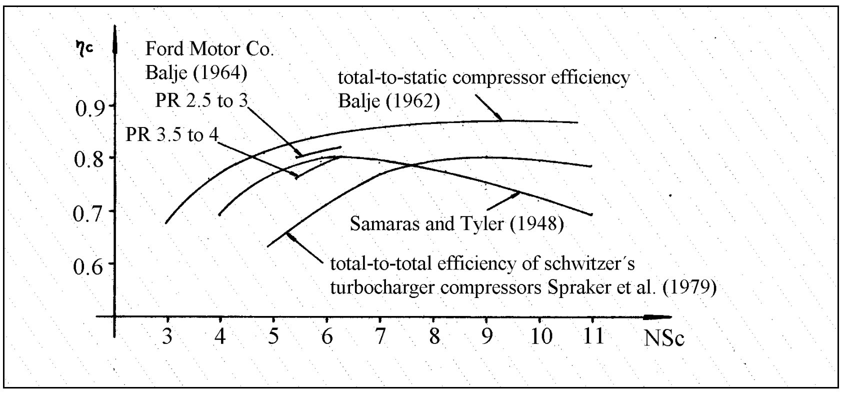

Figure 4. Specific speed versus efficiency correlations. $Ns=rpm\cdot(m^3/s)^{0.5}\cdot(J/kg)^{-0.75}$. To obtain specific speed in U.S. costumary units multiply the values given by 13.47; e.g.: 7.20·13.47=97. Adapted from Spraker et al. (1979).

Rotor slip factor reduces the work done by the centrifugal compressor; various correlations also exist for this factor, which is most dependent on the number of blades. The well-known correlation of Wiesner (1967) was used. These data together with mass flow value yield rotor dimensions to be defined; in Tab. (2) they appear together with other rotor data.

Table 2. Compressor rotor data.

Tip Diameter, mm	60
Inlet Shroud Dia., mm	40
Inlet Hub Dia., mm	15
Tip Width, mm	3.8
Assumed Rotor Isentropic Efficiency	0.88
Slip Factor, σ	0.83
Work Input Parameter, $\Delta H/U_2^2$	0.72
Rotor Relative Velocity Ratio, w_2/w_1	0.58
Specific Speed	7.20

Rotor relative velocity ratio indicates the diffusion taking place within the rotor. Dean (1971) suggests w_2/w_1 (relative velocities at rotor tip and rotor inlet) at 0.56 as the minimum value for unseparated flow at rotor exit; being very close to this value, unseparated flow may occur, suggesting a more efficient operation of the rotor.

The diffuser section employs a piper diffuser unit and no straightening vanes, this type of diffuser has been chosen because of known superior aerodynamic characteristics; as shown for example in Kenny (1969). Although it is normally used in units of higher compression ratio, it makes also a sound structural member. A summary of diffuser data appears in Tab. (3).

Table 3. Diffuser data.

Inner Diameter, mm	66
Outer Diameter, mm	93
Number of Channels	23
Throat Diameter, mm	4
Length of Straight Section, mm	2
Included Angle of Conical Section	14.25°

Compressor wheel stressing was investigated at the maximum rotational speed of 130,000 rpm; see Fig. (5) for results.

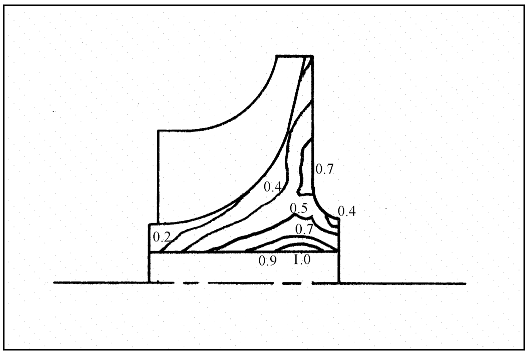

Figure 5. Compressor wheel stresses. Data plotted as regions of constant σ/σ_{max}; at 130,000 rpm, σ_{max}=181 MPa, von Mises equivalent stress. Aluminum alloy A206.0, density 2800 kg/m^3.

As seen from Fig. (5), maximum stress condition occurs in the bore region in the plane of maximum disc diameter, stress level are of a high magnitude and, although they can be handled by high-strength cast aluminum alloys such as A206.0, under the intended application of frequent speed variations, careful attention must be paid to the fatigue problem; a very smooth finish of the rotor bore is one of the measures to be taken to achieve the required cyclic life.

5. Turbine section

An axial flow turbine drives the compressor; in the small gas turbine field, radial turbines are much more often used, for reasons of higher efficiencies, ruggedness, greater tolerance for tip clearances and small sensivity for variations in blade profile. However, units employing radial turbines work at speeds above the first critical unless the bearing next to it is placed very close to the rotor causing it to operate at high temperatures and undergoing even higher temperatures when the unit is shut down and the heat stored in the high mass turbine flows down the shaft.

A radial turbine was considered initially for this project; it had a tip diameter of 56 mm and a mass of 0.115 kg. Later, due to the bearing location issue related above, a decision was taken to substitute an axial turbine for the radial turbine; the resulting design had the same tip diameter of 56 mm and a weight of 0.060 kg, nearly half the value of the radial counterpart. Despite this difference in mass, the two designs had similar polar moments of inertia, this is due to the fact that the radial turbine was of a very "deep scalloped" design, thus concentrating the major part of the mass at lower diameters. A low polar moment of inertia is an important feature in engines subjected to repeated rotational speed excursions.

In jet engines, the energy contained in the exit speed from the turbine wheel is not wasted, as it is in a shaft power unit, thus turbine efficiencies based on total head are used; total-to-total efficiencies of small axial turbines are only slightly lower than in radial counterparts, total-to-static efficiencies are much lower, however.

Geometrical dimensions and other turbine parameters are given in Tab. (4).

Table 4. Axial turbine data.

Tip Diameter, mm	56
Root Diameter, mm	41
Axial Width, mm	6
Number of Blades	29
Axial Solidity at Mean Diameter	1.1
Loading Factor, $\Delta H/U^2$	1.1
Flow Factor, C_x/U	0.7

This stage was designed as to be more loaded in the center of the blade height, the hub and tip producing accordingly less power. It also involved consideration of manufacturing issues such as minimum castable thickness and avoidance of undercuts when viewing from blade tip towards blade base (wheel center) as to permit the use of a single female part in blade/wheel die construction. Assembled compressor and turbine unit appears in Fig. (6).

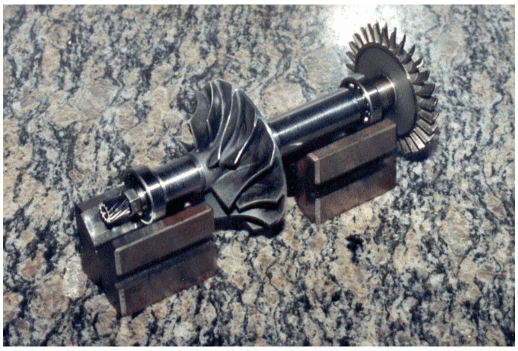

Figure 6. Complete rotating assembly.

Turbine wheel stresses were investigated both at transient and steady state, maximum speed conditions. Stresses in turbine wheel came not only from centrifugal forces but also from significant temperature differences between rim and hub. Analyses were made for wheels having no central hole and for wheels having a central hole of 8 mm, with conditions shown in Fig. (7); results appear in Fig. (8) and Fig. (9).

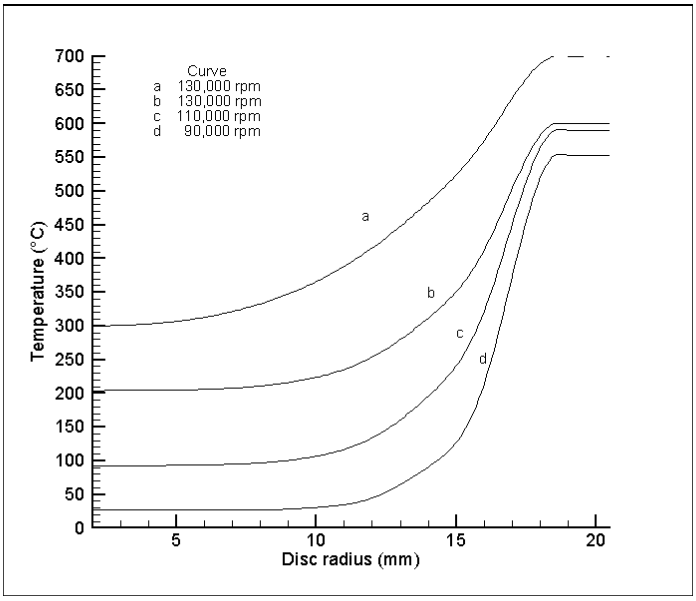

Figure 7. Assumed temperature distribution for stress calculations.

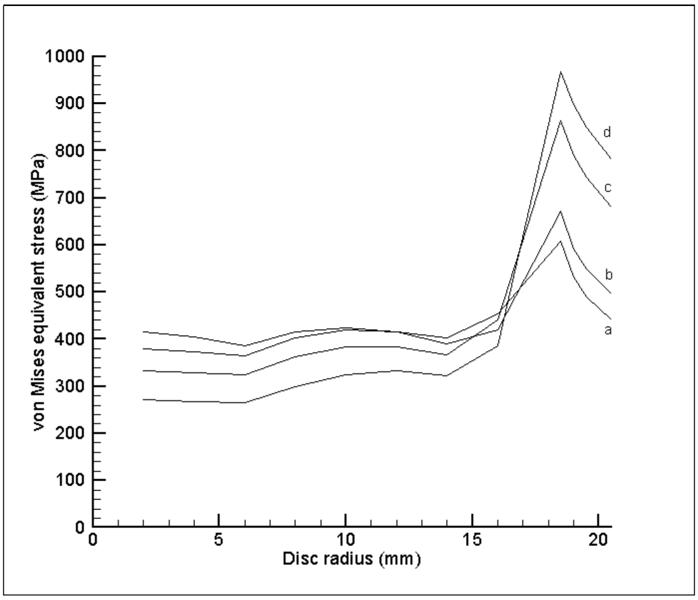

Figure 8. Stresses in turbine wheel having no central hole.

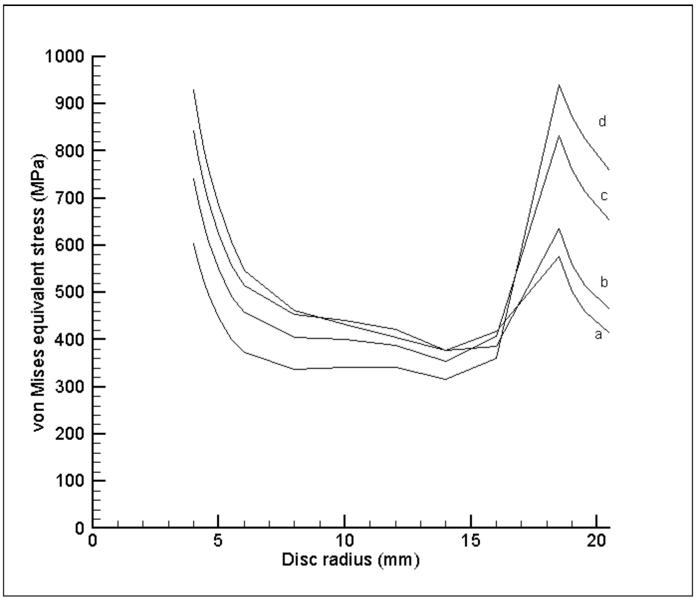

Figure 9. Stresses in turbine wheel having a central hole of 8 mm.

Stresses are shown to be higher near the center of the wheel for the bored version, as one might expect; they are of such a magnitude as to exceed the elastic limit of the material, causing local plastic flow. As pointed out in the introduction section, a life of 200 hours and 50,000 cycles was required; model turbine engines are subjected to a continuous variation of rotational speed, experiencing one complete cycle of idle to full speed to idle again in an average of 15 seconds, this leads to the relatively high number of cycles to happen in a low number of running hours; now, independently of the number of total hours, the unit must be designed to withstand this number of cycles, a detailed analysis of the cyclic life of the bored wheel was not accomplished, but it may well fall below the required life. For production engines, the non-bored version will be employed, this will require the turbine wheel to be friction welded to the shaft; this kind of wheel attachment brings the additional advantage of reducing the heat transfer to the bearing near the turbine wheel by means of a hollow shaft region created around the weld.

Stresses are high also at the rim specially at transient conditions under strong temperature gradients (case d), they are actually compressive stress in the tangential direction and are likely to occur only during the starting phase from rest, cold (ambient temperature) conditions, thus they will occur only once per flight, i.e., with much less frequency than in the case examined above.

6. Combustion section

The unit presented here employs an annular combustion chamber equipped with airblast injectors and a small, conventional spark plug. The combustion chamber is of a high intensity type. Annular height is about 25 mm and it has an overall L/D of 2. Previous use of parameters like these have appeared only in lift engines, where reduced weight and length were more important than high combustion efficiencies. Since compressor discharge directs the air almost entirely towards combustion chamber outer diameter, the single-sided combustor type; described for example in Humenik (1970) or Poyser et al. (1971); appeared to be the most logical layout for this application. In this type of combustor both primary and dilution air are admitted at the outer diameter; thus a single recirculating flow is formed at the primary zone, contrary to the most common types of combustion chamber, where a double, mirrored recirculation pattern is formed; while the inner diameter receives only a small quantity of air mostly for cooling purposes.

A stoichiometric primary zone was chosen as this enables a maximum heat release rate to be obtained; one drawback of the stoichiometric primary zone is the high rate of heat transfer to the combustor walls but this is somewhat counteracted by a high annulus flow speed; furthermore, from scaling considerations, small combustor's walls operate at lower temperatures, see Lefebvre et al. (1959).

Injection is accomplished through a number of airblast injectors. They are of the plain-jet type and are placed at the outer diameter of the combustor; a relatively high combustor pressure drop of $\Delta P_t/P_t$ of 0.05 was made necessary for proper operation down to idle speeds. The atomized fuel issuing from these injectors are directed in an almost tangential direction as to warrant sufficient mixing with primary air.

Although tests performed indicated that light up could be accomplished with these injectors, spool up proved to be completely unsatisfactory, probably due to a combination of improper atomization and a narrow spray angle. For this reason, pressure swirl atomizers are being tried for light-up and initial acceleration up to idle speed at the time of this writing.

The capacitive discharge ignition system consists of charging a capacitor at relatively high voltages, then discharging it rapidly though a small ignition coil in a small conventional spark plug. Although the energy stored in the capacitor reaches 0.5 Joule, preliminary tests performed in a calorimeter have shown that only a very small percentage of this quantity is available as useful heat at the spark plug electrodes. Since only light fuels that are to be used in the operation of this unit such as JP-4 (wide-cut gasoline) or Jet A-1 (kerosene) these reduced energy levels; when compared with full-scale engines; appears to be no disadvantage. Higher energy levels in the ignition system are not being considered for this specific application also for safety reasons. Ignition ability is strongly influenced by quality of atomized fuel and the local mixture strength in the region close to the spark; Fig. (10) shows minimum ignition energy for three sizes of atomized particles (SMD values) and a range of air-fuel ratios from 38:1 to approximately 15:1 (stoichiometric ratio, equivalence ratio =1), thus, besides having to achieve satisfactory atomization, the placement of the ignitor plug in a region of relatively fuel-rich mixture must be carefully analyzed.

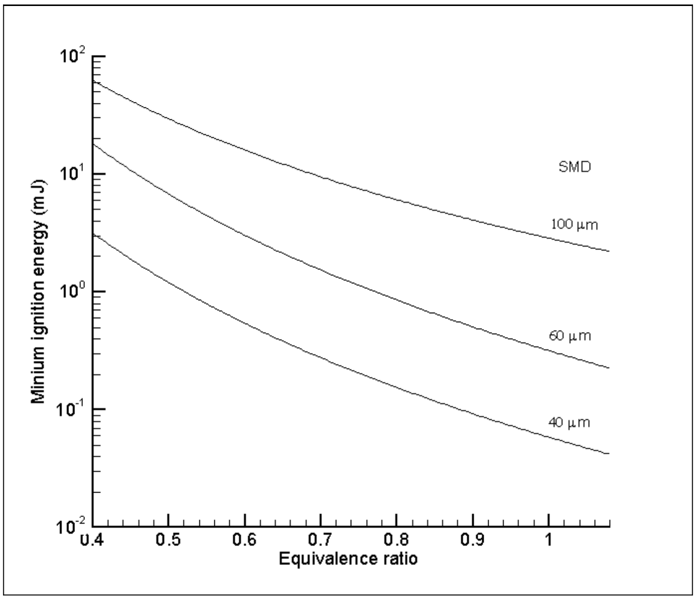

Figure 10. Minimum spark energy levels for ignition in flowing air. Data plotted for isooctane fuel at $P=10^5$ N/m^2, T=17 °C, U=15 m/s. Adapted from Ballal et al. (1979).

7. Rotor dynamics

An analysis was performed using both finite element techniques and matrix-transfer methods to determine the critical bending speeds of the rotating assembly. It was determined that operation should be performed at subcritical speeds, small gas turbines sometimes work at speeds above the 1st or even the 2nd critical speed, specially units having a back-to-back arrangement like that depicted in Fig. (3c), in this case at least one of the bearings are supported in a flexible mounting; in a few cases bearings are rigidly supported and a very strong impingement starting system is employed which makes the unit to pass very rapidly through the critical speeds. In the case presented here the first critical speed was found to be near 140,000 rpm or 7.5% above the maximum operating speed. This is a somewhat slim margin and if this prove to be unsatisfactory modifications will be made; in an extreme case, for example, if it is decided to increase maximum operational speed, calculations indicated that placing the bearing close to the compressor rotor in a flexible support would cause the first critical speed to fall below idle speed and thus increasing the maximum speed above the current level would present no obstacle.

8. Control

The engine control unit (ECU) ensures that parameters like speed and temperatures are within the expected values in all phases of engine operation. The ECU employs electronic circuitry and sensors to interface with the engine, and is powered by energy supplied by the shaft-driven generator, which supplies energy also to the fuel pump, thus making the unit self-sustained and avoiding having to replace/recharge Ni-Cd batteries every time a flight is made. During the starting phase the ECU ensures a correct sequencing of ignition and fuel injection and works as to avoid a hot start, i.e., EGT passing the limit. After idling speed is reached, the unit receives a “throttle lever” signal and translates it into a pulse width modulated (PWM) signal that regulates the fuel pump speed; and thus fuel pump volumetric delivery; ensuring that the unit never surpasses the established speed limit or EGT. During accelerations and decelerations the ECU works to avoid high transient EGTs, blow-outs and compressor surge.

9. Conclusion

Some points covering the design and development of the model 505 small turbojet engine were presented. Design data and selected analysis that were conducted during these phases were discussed along with some experience gained during actual running of the engine. As development is currently active, modifications may occur to fulfill the design goals in terms of performance, safety and reliability.

10. Acknowledgement

I would like to acknowledge Prof. Dr. J. R. Barbosa, Head of Energy Dept., ITA-CTA who kindly reviewed the manuscript.

11. References

Baljé, O.E., 1962, “A Study on Design Criteria and Matching of Turbomachines”, Part B, ASME J. of Engineering for Power, Vol. 84, No.1, pp. 103.

Baljé, O.E., 1964, contribution in Rodgers (1964).

Ballal, D.R. and Lefebvre, A.H., 1979, “Ignition and Flame Quenching of Flowing Heterogeneous Fuel-Air Mixtures”, Combustion and Flame, Vol. 35, No. 2, pp. 155-168.

Dean, R.C., 1971, “On the Unresolved Fluid Dynamics of the Centrifugal Compressors”, in ASME Advanced Centrifugal Compressors, Publication ASME.

Humenik, F.M., 1970, “Performance of a Short Length Turbojet Combustor Insensitive to Radial Distortion of Inlet Airflow”, NASA TN D-5570.

Kenny, D.P., 1969, “A Novel Low-Cost Diffuser for High-Performance Centrifugal Compressors”, ASME J. of Engineering for Power, Vol. 91, No.1., pp. 37-47.

Lefebvre, A.H. and Halls, G.A., 1959, “Some Experiences in Combustion Scaling”, in Advanced Aero Engine Testing, A.W. Morley and J. Fabri (eds.), Joint Meeting of the AGARD Combustion and Propulsion and Wind Tunnel and Model Testing Panels, Copenhagen, October 1958, AGARDograph no. 37, Pergamon Press, pp. 177-203.

Poyser, J.R. and Moxon, H.B., 1971, “The Evolution of the RB 162 Combustion System for VTOL Applications”, in Combustion and Heat Transfer in Gas Turbine Systems, E.R. Norster (ed.), Symposium held at the College of Aeronautics, Cranfield, April 1969, Pergamon Press, pp. 33-62.

Rodgers, C., 1964, “Typical Performance Characteristics of Gas Turbine Radial Compressors”, ASME J. of Engineering for Power, Vol. 86, No.2, pp. 161-175.

Spraker, Jr., W.A. and Chou C.C., 1979, “The Effect of Compressor and Turbine Specific Speed on Turbocharger Efficiency and Engine Performance”, SAE Paper 790065.

Wiesner, F.J., 1967, “A Review of Slip Factors for Centrifugal Impellers”, ASME J. of Engineering for Power, Vol. 89, No. 4, pp. 558-572.